Biochimica et Biophysica Acta 1808 (2011) 1618–1628

Contents lists available at ScienceDirect

Biochimica et Biophysica Acta

journal homepage: www.elsevier.com/locate/bbamem

Spin-echo EPR of Na,K-ATPase unfolding by urea

Rita Guzzi [a], Mohammad Babavali [a,b], Rosa Bartucci [a], Luigi Sportelli [a], Mikael Esmann [b], Derek Marsh [c,*]

[a] Dipartimento di Fisica and UdR CNISM, Università della Calabria, 87036 Arcavacata di Rende (CS), Italy
[b] Department of Physiology and Biophysics, Aarhus University, Aarhus, Denmark
[c] Max-Planck-Institut für biophysikalische Chemie, Abt. Spektroskopie, 37077 Göttingen, Germany

ARTICLE INFO

Article history:
Received 24 September 2010
Received in revised form 3 November 2010
Accepted 3 November 2010
Available online 10 November 2010

Keywords:
Denaturation
Spin label
SH groups
Echo-detected EPR
ESEEM
Librations
Solvation

ABSTRACT

Denaturant-perturbation and pulsed EPR spectroscopy are combined to probe the folding of the membrane-bound Na,K-ATPase active transport system. The Na,K-ATPase enzymes from shark salt gland and pig kidney are covalently spin labelled on cysteine residues that either do not perturb or are essential to hydrolytic activity (Class I and Class II –SH groups, respectively). Urea increases the accessibility of water to the spin-labelled groups and increases their mutual separations, as recorded by D_2O interactions from ESEEM spectroscopy and instantaneous spin diffusion from echo-detected EPR spectra, respectively. The greater effects of urea are experienced by Class I groups, which indicates preferential unfolding of the extramembrane domains. Conformational heterogeneity induced by urea causes dispersion in spin-echo phase-memory times to persist to higher temperatures. Analysis of lineshapes from partially relaxed echo-detected EPR spectra indicates that perturbation by urea enhances the amplitude and rate of fluctuations between conformational substates, in the higher temperature regime, and also depresses the glasslike transition in the protein. These non-native substates that are promoted by urea lie off the enzymatic pathway and contribute to the loss of function.

1. Introduction

The Na,K-ATPase active transport enzyme is an integral protein of the plasma membrane that is responsible for maintaining ionic homeostasis in eukaryotes. The α-subunit has a multiple-spanning transmembrane sector, with associated single-spanning accessory and regulatory β- and γ-subunits, and a large, globular cytoplasmic sector that contains the nucleotide-binding and hydrolytic sites [1–3]. The analogous P-type Ca-ATPase of the sarcoplasmic or endoplasmic reticulum (SERCA) is similar in structure to the α-subunit of the Na,K-ATPase [1,2].

Perturbation by aqueous denaturants affords a valuable means to probe the folding of globular and membrane proteins [4–10]. For instance, both infrared spectroscopy and activity measurements have been used to study denaturant-mediated unfolding of the SERCA Ca-ATPase [11,12]. Fig. 1 illustrates the urea-induced unfolding of Na,K-ATPase from two different species, as monitored by conventional continuous-wave electron paramagnetic resonance (CW-EPR)[1] spectroscopy of a maleimide spin label covalently attached to Class II [13] cysteine residues [14]. Unfolding of those domains of the membranous protein that are accessible to urea results in conversion to a weakly immobilized (*W*) state of spin-labelled residues, which, in the native protein, are strongly immobilized (*S*) on the conventional EPR timescale. The sigmoidal dependence on denaturant concentration reflects the cooperative nature of the unfolding transitions. The effects of urea on the CW-EPR spectra are completely reversible [14], reflecting reversible structural changes associated with the folding/unfolding process.

Recently, we have shown that the combination of conventional CW-EPR with spin-echo EPR spectroscopy [15] can be used to characterize the conformational heterogeneity of the Na,K-ATPase [16]. Conformational substates [17,18], which are frozen in at low temperatures, are detected by inhomogeneous broadening of the CW-EPR spectra and dispersion in phase-memory relaxation times of the spin-labelled protein. Motional averaging of these conformational substates is driven by librational fluctuations that are observed by echo-detected EPR spectra. In addition, modulation of the spin-echo decays by hyperfine interaction with D_2O (^{2}H-ESEEM) was shown to reveal the differential accessibility to water of different classes of spin-labelled –SH groups in the Na,K-ATPase.

In the present work, we use this combination of CW-EPR and pulsed EPR to investigate the urea-induced unfolding of membranous Na,K-ATPase from both shark salt gland and pig kidney. D_2O-ESEEM quantifies the increase in exposure to water of those parts of the protein that are unfolded in urea. ED-EPR spectra detect the onset of librational motions that drive transitions between conformational substates. Echo decay rates probe the increase in conformational heterogeneity that is induced by urea. Deconvolution of the CW-EPR lineshapes shows the effect of urea on motional averaging of the on-pathway substates. In addition, ED-EPR spectra at low temperature,

* Corresponding author. Tel.: +49 551 201 1285/+49 551 201 1501.
E-mail address: dmarsh@gwdg.de (D. Marsh).

0005-2736/$ – see front matter © 2010 Elsevier B.V. All rights reserved.
doi:10.1016/j.bbamem.2010.11.008

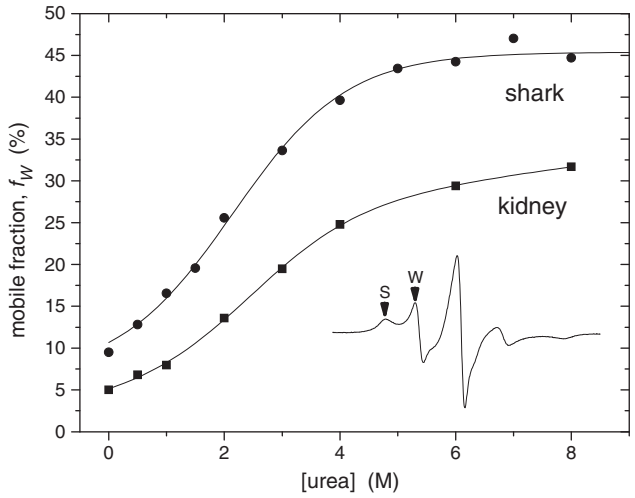

Fig. 1. Fraction, f_W, of weakly immobilized component in the CW-EPR spectra of shark salt gland (circles) and pig kidney (squares) Na,K-ATPase spin labelled with 5-MSL (pH 7.4), as a function of urea concentration, at 4 °C. 5-MSL is covalently bound to Class II sulphydryl groups. Inset: CW-EPR spectrum of shark Na,K-ATPase in 1 M urea; W and S indicate the weakly and strongly immobilized components, respectively. Data are from Ref. [14].

which are sensitive to instantaneous diffusion that arises from mutual spin–spin interactions, reveal the extension of the polypeptide structure that results from urea-induced unfolding.

2. Materials and methods

2.1. Enzyme preparation

The Na,K-ATPase membranes from pig kidney and shark salt gland were prepared as described earlier [19,20]. Specific activities were 28 and 32 μmol P_i generated per milligram protein per minute at 37 °C, for kidney and shark preparations, respectively. The shark enzyme was stored at a protein concentration of approx. 5 mg/ml in 20 mM histidine and 25% glycerol (pH 7.0) and the kidney enzyme at a protein concentration of approx. 4 mg/ml in 20 mM histidine, 250 mM sucrose, and 1 mM EDTA (pH 7.0). Protein concentrations were determined by using the Lowry method [21], and enzymatic assays were performed as described previously [22].

2.2. Spin labelling of Na,K-ATPase membranes

Prelabelling of shark Na,K-ATPase with NEM to block Class I –SH groups, and sulphydryl groups of non-Na,K-ATPase proteins in the membrane preparations, was performed as described previously (see Refs. [16] and [23] for details). The prelabelled shark enzyme had more than 95% of the initial specific activity and was stored in 20 mM histidine and 25% (v/v) glycerol at −20 °C. Prelabelling of kidney Na,K-ATPase followed the same route (see Ref. [16] for details). The prelabelled kidney enzyme had more than 90% of the initial specific activity and was stored at −20°C in 20 mM histidine, 250 mM sucrose, and 1 mM EDTA (pH 7.0).

Class I –SH groups in the Na,K-ATPase membranes were spin labelled with 5-MSL (3-maleimido-1-oxyl-2,2,5,5-tetramethylpyrrolidine; Sigma, St. Louis, MO) by using the same protocol as that for prelabelling with NEM. For shark enzyme, the native membranes were treated with 0.2 mM 5-MSL, and the spin-labelled enzyme had more than 95% of the initial specific activity. For kidney enzyme, a spin label concentration of 1.25 mM was used, and the spin-labelled enzyme had more than 90% of the initial specific activity.

Selective spin labelling of the Class II –SH groups, which are essential to the overall Na,K-ATPase activity, was performed with NEM-prelabelled enzyme in the presence of 3 mM ATP as described previously [13,16]. The concentration of 5-MSL used was 0.125 mM for shark enzyme and 1.0 mM for kidney, resulting in residual activities of 8% and 20%, respectively.

2.3. Deuterium exchange of spin-labelled membranes

A buffer was prepared by using D_2O containing the following salts: 11 mM Tris, 11 mM CDTA, and 22 mM NaCl (pH 7.0 at 20 °C). 5-MSL spin-labelled Na,K-ATPase (see above) was pelleted by centrifugation, and approximately 15 mg protein was homogenized in 10 ml of the D_2O buffer. This membrane suspension was incubated at 14 °C for 60 min and pelleted by centrifugation at 100,000×g for 2 h at 14 °C. The pellet was homogenized in 10 ml of the D_2O buffer and incubated at 14 °C for 12 h, after which it was pelleted by centrifugation as above. Samples in H_2O were subjected to the same manipulations as the D_2O samples.

2.4. Treatment of spin-labelled membranes with urea

The pellets after D_2O or H_2O treatment (see preceding paragraph) were weighed, and solid urea was homogenized with the pellet to give final concentrations of 2.5 or 5 M (it was assumed that the pellet as well as the final sample had a density of 1 g/ml). For samples in H_2O buffer, normal urea was used and, for samples in D_2O buffer, fully deuterated urea was used ($[^2H]_4$ urea, Cambridge Isotope Laboratories, MA). Samples without urea were treated as those with urea. The samples were incubated overnight at 14 °C and then transferred to quartz EPR tubes (inner diameter 3 mm) with a sample volume of ca. 100 μl and stored at −20 °C.

2.5. EPR spectroscopy

Pulsed EPR data were collected on an ELEXSYS E580 9-GHz Fourier Transform FT-EPR spectrometer (Bruker, Karlsruhe, Germany) equipped with a MD5 dielectric resonator and a CF 935P cryostat (Oxford Instruments, UK).

To obtain ESEEM spectra, three-pulse, stimulated echo ($\pi/2$–τ–$\pi/2$–T–$\pi/2$–τ–echo) decays were collected by using microwave pulse widths of 12 ns, with the microwave power adjusted to give $\pi/2$ pulses. The time delay T between the second and the third pulses was incremented from 20 ns by 700 steps of $\Delta T = 12$ ns, while maintaining the separation τ between the first and the second pulses constant at 168 ns. A four-step phase-cycling program, $+(x,x,x)$, $-(x,-x,x)$, $-(-x,x,x)$, $+(-x,-x,x)$, where the initial sign indicates the phase of the detection ($\pm y$), was used to eliminate unwanted echoes. The magnetic field was set to the maximum of the EPR absorption. The time-dependent echo amplitudes, $V(\tau,T)$, were processed to yield standardized ESEEM intensities, according to the protocol developed previously [24,25]. The average experimental echo decay, $\langle V(\tau,T)\rangle$, was fitted with a biexponential function. The normalized ESE modulation signal was then obtained as:

$$V_{norm}(\tau,T) = V(\tau,T) / \langle V(\tau,T)\rangle - 1 \quad (1)$$

Three levels of zero filling were added to increase the total number of points to 4 K. The absolute-value ESEEM spectrum was then calculated, with specific inclusion of the dwell time ($\Delta T = 12$ ns) between points, yielding standardized intensities with dimensions of time [25].

By application of the mass-action law, the product of the equilibrium constant, K, for H-bonding and the effective concentration, $[W]$, of free water is related to the normalized intensity, I_{broad}, of the broad D_2O-ESEEM component by [24]:

$$K[W] = \frac{I_{broad} / I_o}{2 - I_{broad} / I_o} \quad (2)$$

where I_o ($\approx$115 ns) is the normalized ^{2}H-ESEEM intensity for a nitroxide with a single hydrogen-bonded D_2O molecule that is predicted by DFT calculations [24]. Correspondingly, the fraction of spin-labelled –SH groups that is H-bonded by a single water molecule is given by [24]:

$$f_{1W} = \frac{2}{1/K[W] + 2 + K[W]} \tag{3}$$

The fraction of spin-labelled –SH groups that is H-bonded by two water molecules is then given by:

$$f_{2W} = \frac{1}{2}\left(\frac{I_{broad}}{I_o} - f_{1W}\right) \tag{4}$$

Eqs. (2–4) are all based on quantification of the broad D_2O-ESEEM component, which has been shown by quantum-chemical calculations to arise from nitroxides with directly H-bonded D_2O molecules.

Two-pulse ($\pi/2$–τ–π–τ–echo) spin-echo decays were obtained by integrating the echo and incrementing the pulse spacing, τ. The window for the integration was 120 ns. The microwave pulse widths were 32 ns and 64 ns, with the microwave power adjusted to provide $\pi/2$ and π pulses, respectively. The magnetic field was again set to the EPR absorption maximum. The τ dependence of the integrated echo intensity, $I(\tau)$, was fitted with a double exponential decay function:

$$I(\tau) = I_1(0)\ exp\left(-2\tau / T_{2M,1}\right) + I_2(0)\ exp\left(-2\tau / T_{2M,2}\right) \tag{5}$$

where $T_{2M,i}$ are the phase-memory times of the different components and $I_i(0)$ are their respective intensities.

Partially relaxed two-pulse ($\pi/2$–τ–π–τ–echo) echo-detected EPR spectra were obtained by recording the integrated spin-echo signal at fixed interpulse delay τ, while sweeping the magnetic field. The microwave pulse widths were the same as those used for recording the echo decays, and the integration window was 160 ns. The original ED spectra, $ED_T(2\tau,H)$, were corrected for instantaneous spin diffusion by normalizing with respect to those recorded at 77 K, where no molecular motion is expected. The corrected spectra, $ED_T^{corr}(2\tau,H)$, recorded at temperature T are plotted as a function of magnetic field, H, according to Ref. [26]:

$$ED_T^{corr}(2\tau,H) = ED_T(2\tau,H)\frac{ED_{77K}(2\tau_0,H)}{ED_{77K}(2\tau,H)} \tag{6}$$

where τ_0 is the shortest value of τ for which ED spectra were obtained. Relaxation rates, $W(H,\tau_1,\tau_2)$, were determined from the ratio of corrected ED spectra recorded at two different values, τ_1 and τ_2, of the interpulse delay by using the following relation [27]:

$$W(H,\tau_1,\tau_2) = ln\left[\frac{ED(2\tau_1,H)}{ED(2\tau_2,H)}\right]\cdot\frac{1}{2(\tau_2-\tau_1)} \tag{7}$$

where $ED(2\tau,H)$ is the ED spectral line height at field position H. These relaxation rates are averaged over the time interval from τ_1 to τ_2 and are characterized by the maximum values, W_L and W_H, determined in the low- and high-field regions, respectively, of the ED spectra. Calibration of the W_L and W_H relaxation rates in terms of the amplitude-correlation time product, $\langle\alpha^2\rangle\tau_c$, of rotational motion from low-amplitude librations is taken from the results of spectral simulations [26–28]. Here, α is the angular amplitude, τ_c is the correlation time, and angular brackets indicate an average over the librational motion.

Partially relaxed, three-pulse ($\pi/2-\tau-\pi/2-T-\pi/2-\tau-$echo), stimulated echo-detected EPR spectra, $ED_{SE}(T,H)$, were obtained by recording the integrated spin-echo signal at fixed interpulse delays τ and T, while sweeping the magnetic field. Corresponding inversion recovery ($\pi-T-\pi/2-\tau-\pi-\tau-$echo) echo-detected EPR spectra, $ED_{IR}(T,H)$, were obtained in a similar manner. In each case, the integration window and the microwave pulse widths were the same as those used for the two-pulse $ED(2\tau,H)$ spectra. The original three-pulse ED spectra were corrected for spin-lattice relaxation by using the inversion recovery ED spectra [26]:

$$ED_{SE}^{corr}(T,H) = ED_{SE}(T,H)\frac{\Delta ED_{IR}(0,H)}{\Delta ED_{IR}(T,H)} \tag{8}$$

where $\Delta ED_{IR}(T,H) = ED_{IR}(\infty,H) - ED_{IR}(T,H)$. The spectrum for $T=\infty$ was obtained with the first pulse turned off and, for $T=0$, we take $ED_{IR}(0,H) = -ED_{IR}(\infty,H)$.

Conventional CW EPR spectra were recorded on an ESP-300 9-GHz spectrometer (Bruker, Karlsruhe, Germany) using 100-kHz field modulation; the spectrometer was equipped with an ER 4111VT temperature controller. The low-field ($m_I = +1$) hyperfine extremum in the CW-EPR powder patterns from random membrane dispersions was fitted by non-linear least-squares minimization with a Voigt absorption lineshape:

$$v(H) = A\int_{-\infty}^{\infty}\frac{exp\left(-(H'-H_o)^2/2\Delta H_G^2\right)}{(\Delta H_L/2)^2 + (H-H')^2}dH' \tag{9}$$

where ΔH_L is the half-width at half-height of each Lorentzian component, ΔH_G is the width of the Gaussian distribution of Lorentzian components, and H_o is the center of the Gaussian distribution. The high-field wings were omitted from the fitting procedure to eliminate any distortion by the powder pattern envelope.

3. Results

First we describe the influence of urea on water accessibility of the spin-labelled protein, as determined by ESEEM spectroscopy. Next we use echo-detected spectra at low temperature to study the effect of urea-induced unfolding on internal spin–spin interactions. Then we describe the use of conventional CW-EPR lineshapes to study heterogeneity of protein substates at low temperature. Finally, we use partially relaxed, echo-detected EPR spectra to study the effect of urea on librational fluctuations of the protein.

3.1. D_2O-ESEEM spectra

Fig. 2 shows the absolute-value ESEEM spectra of shark and kidney Na,K-ATPase samples that are spin labelled on Class I or Class II –SH groups with 5-MSL and are suspended in D_2O buffer, with or without urea. All spectra consist of a peak at the ^{2}H-Larmor frequency of ca. 2.6 MHz that arises from D_2O in the vicinity of the spin-labelled groups and a peak at the ^{1}H-Larmor frequency of 14.6 MHz that arises from matrix protons and serves as an additional internal standard for the D_2O intensity. The D_2O peak of each spectrum consists of a broad component that arises from D_2O molecules that are hydrogen-bonded to the nitroxide and a narrow component that corresponds to D_2O molecules, which are not H-bonded to the –NO group but are located in the vicinity of the spin-label site [24].

Fig. 3 gives the standardized intensities of the total D_2O-ESEEM spectrum and of the broad (H-bond) component for the different samples. In all cases, the D_2O-ESEEM intensities increase in the presence of urea, relative to in its absence. This corresponds to an increased accessibility of the spin-labelled Class I and Class II –SH groups to water in the urea-unfolded state of the enzyme from either species. However, the ratio of the intensity of the broad component to that of the total spectrum decreases in the presence of urea. Evidently, urea partially disrupts hydrogen bonding of water to the nitroxide resulting in a smaller net effect on the broad component. In 5 M urea, the D_2O-ESEEM intensities of kidney Class I groups notably are greater

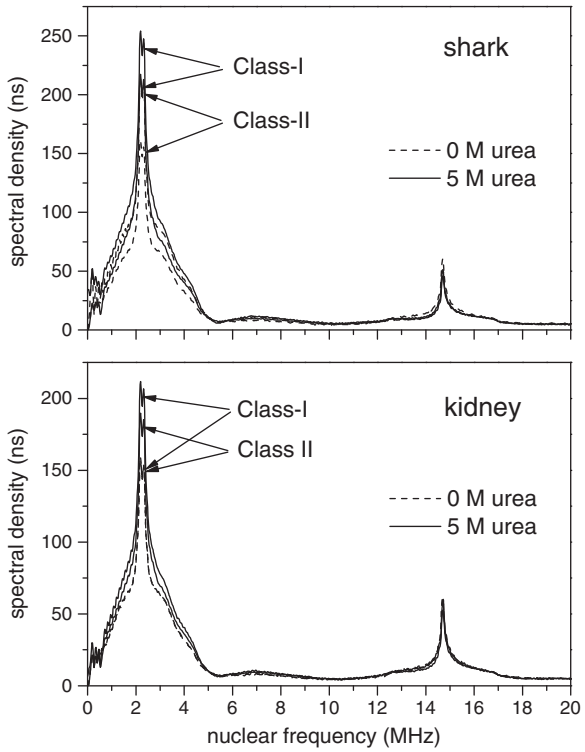

Fig. 2. Absolute-value ESEEM spectra of shark salt gland (upper panel) and pig kidney (lower panel) Na,K-ATPase spin labelled with 5-MSL on Class I or Class II –SH groups, as indicated, in the presence (solid lines) and absence (dashed lines) of 5 M urea. For the shark enzyme, the spectrum of Class I groups in the absence of urea overlaps that for Class II groups in the presence of urea. For the kidney enzyme in the absence of urea, the spectra of Class I and Class II groups practically superimpose.

than those of Class II groups, although in the absence of urea the two are indistinguishable.

Table 1 lists the values of $K[W]$, f_{1W} and f_{2W}, which characterize the H-bonding of water to the spin-label –NO groups. These parameters are obtained from the D_2O-ESEEM data by using Eqs. (2–4), for Class I and Class II groups of shark and kidney Na,K-ATPases, in the presence and absence of urea. Unfolding by urea increases the average fraction of spin-labelled –SH groups that are available for H-bonding with water, even though, as already noted, urea reduces the intrinsic propensity of the spin label to H-bond with water.

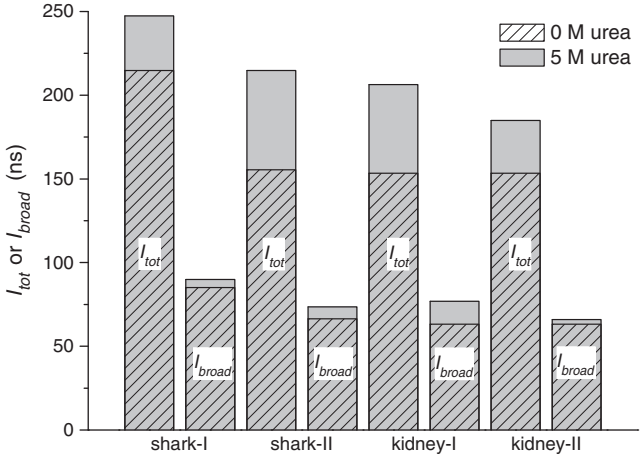

Fig. 3. Total D_2O-ESEEM intensities (I_{tot}, left hand of each pair) and intensities of the broad D_2O-ESEEM component (I_{broad}, right hand of each pair) for shark salt gland and pig kidney Na,K-ATPase spin labelled with 5-MSL on Class I or Class II –SH groups, as indicated, in the presence (grey) and absence (hatched, light grey) of 5 M urea.

Table 1
Normalized intensities, fractions of spin-labelled Class I and Class II –SH groups in shark or pig kidney Na,K-ATPase that are hydrogen bonded by one (f_{1W}) and two (f_{2W}) water molecules, and product of the equilibrium constant for H-bonding, K, with the effective free water concentration, $[W]$, from ^{2}H-ESEEM spectra of D_2O-membrane dispersions in the presence of the concentrations of urea indicated.[a]

[Urea] (M)	I_{broad}/I_o	K [W]	f_{1W}	f_{2W}
Shark Class I:				
0	0.75	0.60	0.47	0.14
2.5	0.93	0.87	0.50	0.22
5	0.79	0.65	0.48	0.16
Shark Class II:				
0	0.58	0.41	0.41	0.09
5	0.65	0.48	0.44	0.10
Kidney Class I:				
0	0.55	0.38	0.40	0.08
5	0.67	0.51	0.45	0.11
Kidney Class II:				
0	0.55	0.38	0.40	0.08
5	0.58	0.41	0.41	0.08

[a] Deduced from Eqs. (2–4). $I_o = 115$ ns is the quantum-chemical estimate of I_{broad} for H-bonding with one water molecule [24].

3.2. Two-pulse echo-detected (ED) EPR spectra at 77 K

Fig. 4 shows the two-pulse ED-EPR spectra of spin-labelled Na,K-ATPase preparations in the presence and absence of urea at 77 K. At this low temperature, molecular motion is suppressed but the ED-EPR spectra are sensitive to spin–spin interactions, which cause the so-called instantaneous diffusion [26]. These spectra are therefore a useful means to detect magnetic dipolar interactions between different spin labels on the same protein or, in the case of aggregation, between different proteins. Instantaneous diffusion characteristically causes the central region of the spectrum to decay faster with increasing echo delay time, τ, than do the outer wings [29,30]. It is remarkable that spin-labelled kidney Class II groups exhibit relatively little instantaneous spin diffusion, both in the presence and absence of urea, whereas the spectral lineshape changes considerably with increasing τ for the other spin-labelled Na,K-ATPase preparations.

The line height of the central peak in the ED spectra, relative to that at low-field, (C/L) is a sensitive monitor of instantaneous diffusion [31]. According to the theory of instantaneous diffusion [30,32], the dependence of C/L on echo decay time τ takes the form:

$$C/L(\tau, c_{SL}) = (C/L)_o \, exp(-k_{id}(c_{SL})\tau) \quad (10)$$

where $k_{id}(c_{SL})$ is an effective rate constant for instantaneous diffusion, which is linearly proportional to the spin-label concentration, c_{SL}, for a uniform spatial distribution of spins. Preferential interaction between spin labels is therefore reflected by an increase in the value of k_{id}. Fig. 5 gives the rate of instantaneous diffusion for shark and kidney Na,K-ATPase spin labelled on either Class I or Class II –SH groups, in the presence and absence of urea. The inset to Fig. 5 shows typical decay curves for the C/L line height ratio with increasing τ. For Class I groups of both shark and kidney, the values of k_{id} are smaller in the presence of urea than in its absence. This corresponds to a decrease in spin–spin interactions for the partially unfolded enzymes in urea. The most likely explanation for this is that the spin–spin interactions giving rise to instantaneous diffusion are intramolecular, between spin labels on the same enzyme molecule, and that in the unfolded state, these labels are more widely separated because the structure becomes more extended. For Class II groups, on the other hand, the

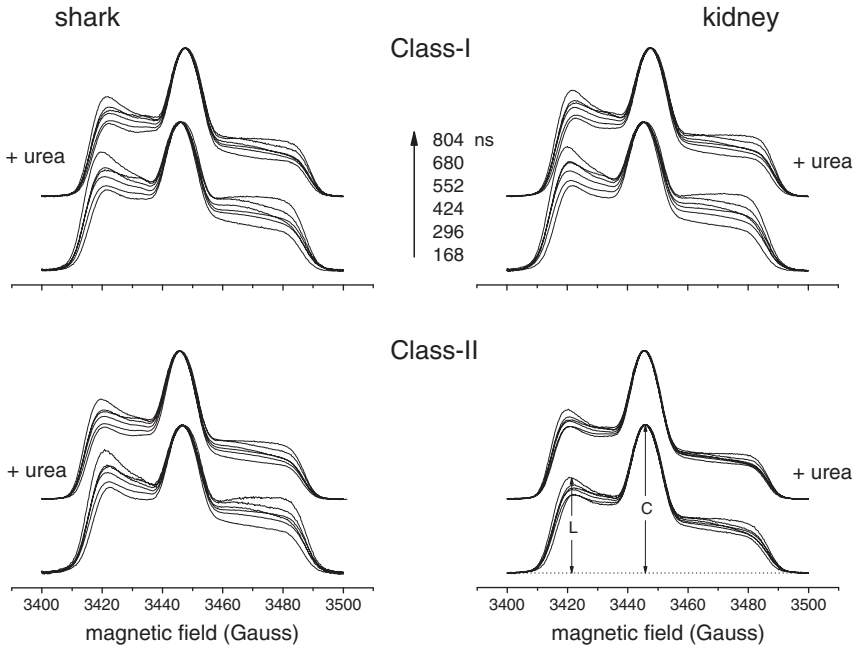

Fig. 4. Two-pulse echo-detected EPR spectra at 77 K, as function of echo delay time, for shark salt gland (left-hand side) and pig kidney (right-hand side) Na,K-ATPase spin labelled with 5-MSL on Class I (upper panel) or Class II (lower panel) –SH groups, in the presence and absence of 5 M urea, as indicated. ED spectra are recorded for interpulse spacings of (bottom to top) $\tau = 168$, 296, 424, 552, 680, and 804 ns. Spectra are normalized to the central peak (C); the low-field maximum (L) is also indicated.

values of k_{id} differ only slightly in the presence and absence of urea. Possibly, the spin labels on Class II groups are relatively situated such that their separation does not change greatly on unfolding by urea. As already noted, the instantaneous diffusion rates of kidney Class II groups are inherently low.

3.3. Spin-echo decays and phase-memory times

Fig. 6 shows the temperature dependence of the phase-memory time T_{2M} for Na,K-ATPase preparations labelled on Class I (upper panels) or Class II (lower panels) –SH groups with 5-MSL and suspended in 5 M urea (solid lines and symbols). For comparison, corresponding data for Na,K-ATPase without urea from Ref. [16] are given by dashed lines and open symbols in Fig. 6. It was found previously that, at temperatures below 150 K, a double exponential function was needed to describe the echo decays of spin-labelled Na,K-ATPase in the absence of urea. At higher temperatures, a single exponential was found to be adequate (see open symbols in Fig. 6). The phase-memory times for Na,K-ATPase in the presence of urea were obtained by fitting the experimental echo decay curves with Eq. (5) for a double exponential (see solid symbols in Fig. 6). It is found that, in the presence of urea, the heterogeneity in phase-memory times extends to considerably higher temperatures than in the absence of urea. For preparations in urea, the echo decays can be described by a single exponential function (which corresponds to a single phase-memory time) only at temperatures of 210—240 K and above.

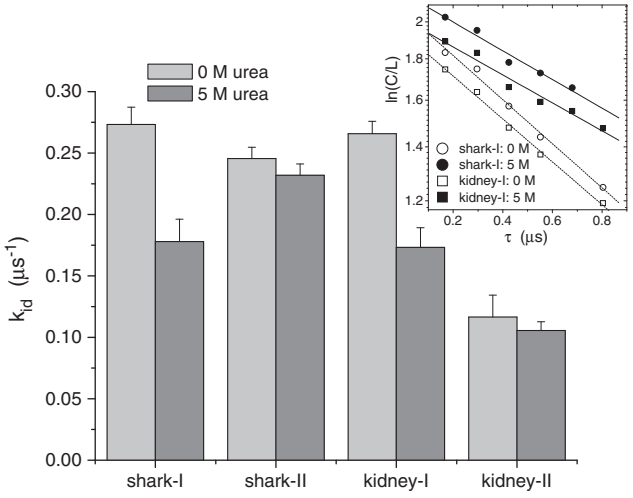

Fig. 5. Rate of instantaneous diffusion, k_{id}, for shark salt gland and pig kidney Na,K-ATPase spin labelled with 5-MSL on Class I or Class II –SH groups, in the presence and absence of 5 M urea, as indicated. Rates are determined from single-exponential fits (see Eq. (10)) of the decay with echo delay time, τ, of the central to low-field line height ratio (C/L) in ED-EPR spectra at 77 K, as shown in the inset, which has a logarithmic ordinate.

3.4. Continuous-wave (CW) EPR spectra

Fig. 7 shows the temperature dependence of CW-EPR spectra from 5-MSL-labelled Class II –SH groups of shark Na,K-ATPase in the presence (solid lines) and in the absence (dashed lines) of 5 M urea. In all cases, the spectral lines are narrower in the presence of urea than in its absence. Also, the outer hyperfine splittings, $2A_{zz}$, are smaller in the presence of urea than in its absence. The powder patterns that are obtained at low temperature are characterized by inhomogeneously broadened lineshapes with partial Gaussian character. With increasing temperature, the lines narrow progressively and the lineshapes become more homogeneous until finally they achieve almost pure Lorentzian shape. The crosses in Fig. 7 represent fitting of Voigt absorption lineshapes (which correspond to a Gaussian convolution of pure Lorentzian components, see Eq. (9)) to the low-field hyperfine extremum.

Fig. 8 shows the temperature dependences of the widths of the Gaussian distribution (ΔH_G) and of the Lorentzian components (ΔH_L) that are obtained by fitting the CW-EPR spectra of Class I and Class II groups of the shark and kidney Na,K-ATPases (cf. Fig. 7). In the presence of urea, the Lorentzian linewidths are less than those in the absence of urea, for both shark and kidney enzymes. On the other hand, the Gaussian linewidths at low temperatures are slightly larger

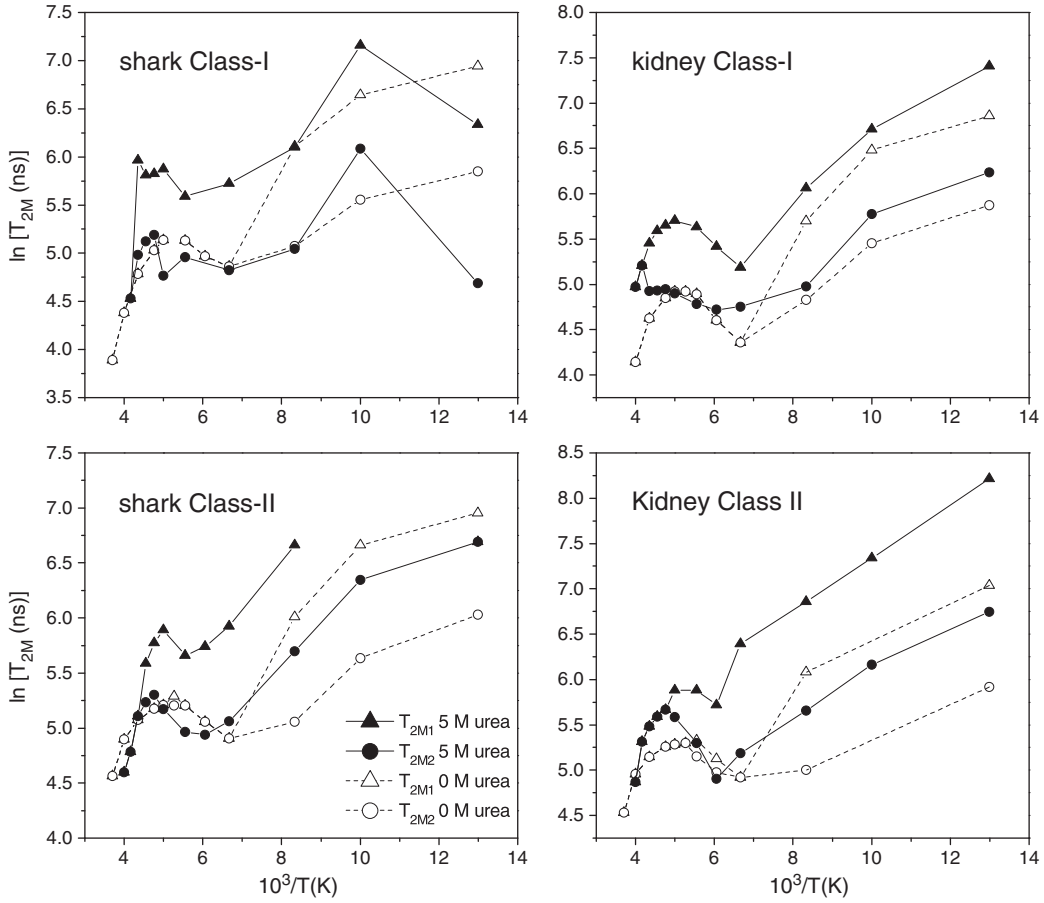

Fig. 6. Temperature dependence of the phase-memory time, T_{2M}, for 5-MSL-labelled Class I (upper panels) or Class II (lower panels) –SH groups of shark salt gland (left panels) and pig kidney (right panels) Na,K-ATPase, in the presence (solid symbols) and absence (open symbols) of 5 M urea. Circles and triangles are from double-exponential fits (Eq. (5)) to the echo decay curves. Data for Na,K-ATPase in the absence of urea are from Ref. [16].

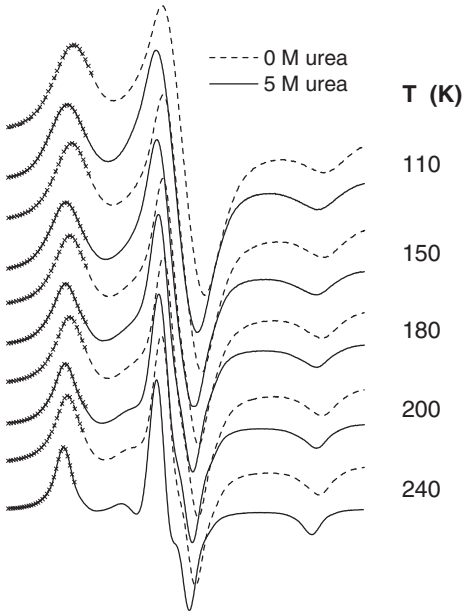

Fig. 7. Temperature dependence of the CW-EPR spectra of 5-MSL-labelled Class II –SH groups of shark salt gland Na,K-ATPase, in the presence (solid lines) and the absence (dashed lines) of 5 M urea. Crosses represent fitting of the low-field ($m_I = +1$) hyperfine extremum with a Voigt lineshape (Eq. (9)). Total scan width = 100 Gauss.

in the presence of urea than in the absence of urea. Both Lorentzian and Gaussian linewidths of the shark enzyme are more similar to those of the kidney enzyme in the presence of urea than are found for the two native Na,K-ATPases in the absence of urea. The Lorentzian linewidths decrease only slowly with increasing temperature, both in the presence and absence of urea. In contrast, the widths of the Gaussian distributions decrease progressively already from the lowest temperatures, reaching zero or rather low values at temperatures above 220 K in the presence of urea.

Fig. 10B and D shows the temperature dependences of the outer hyperfine splitting, $2\langle A_{zz}\rangle$, for the CW-EPR spectra of both shark and kidney Na,K-ATPase spin labelled on Class I or Class II groups, in the presence of 5 M urea (Fig. 10 is given later, where it includes corresponding data from ED-EPR). Initially, at low temperatures, the effective hyperfine splittings are approximately constant. This corresponds to the temperature regime over which the inhomogeneous broadening is appreciable (cf. Fig. 8). Under these conditions, the hyperfine splittings correspond to their rigid-limit values, $2A_{zz}$, which are dependent solely on the polarity of the spin-label environment (see, e.g., 33,34). Whereas in the absence of urea, the polarity of shark Class I groups is greater than those of kidney Na, K-ATPase [16], in the urea-unfolded state, they become comparable.

Above 200—220 K, the values of $2\langle A_{zz}\rangle$ decrease steeply with increasing temperature, as a result of progressive motional narrowing by rapid, small-amplitude torsional librations [35]. At a given temperature in this dynamic regime, the decrease in $2\langle A_{zz}\rangle$ is greater in the presence of urea than in its absence (cf. 16), and this effect is larger for the kidney enzyme than for the shark enzyme. Interestingly, the values of $2\langle A_{zz}\rangle$ converge at the melting point of the aqueous medium, which is reduced to 250 K in the presence of 5 M urea.

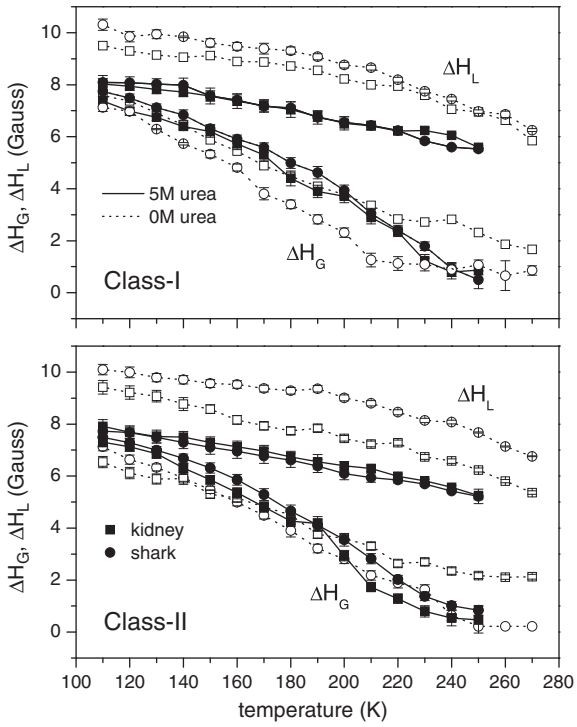

Fig. 8. Temperature dependence of the Gaussian (ΔH_G, four lower traces) and Lorentzian (ΔH_L, four upper traces) widths of the low-field ($m_I = +1$) hyperfine line obtained by fitting Voigt lineshapes (Eq. (9)) to the CW-EPR spectra of 5-MSL-labelled Class I (upper panel) or Class II (lower panel) –SH groups of shark salt gland (circles) and pig kidney (squares) Na,K-ATPase in the presence (solid lines and solid symbols) and absence (dotted lines and open symbols) of 5 M urea.

3.5. Two-pulse echo-detected EPR spectra

Fig. 9 shows the two-pulse, echo-detected (ED) EPR spectra of shark (left-hand side) and kidney (right-hand side) Na,K-ATPase preparations that are spin labelled on Class I (upper panel) or Class II (lower panel) –SH groups with 5-MSL, in the presence of 5 M urea. The spectra are recorded at 210 K and are given for increasing values of the echo delay time, τ. The dependence of the corrected ED lineshapes on the τ delay reveals preferential relaxation in the intermediate spectral regions at low and high field that is characteristic of rapid, small-amplitude torsional librations [36,37]. The corresponding relaxation spectra, as defined by Eq. (7), are given underneath the ED spectra in Fig. 9. *W*-relaxation spectra evaluated for different pairs of τ_1 and τ_2 coincide to within the noise level, showing that the relaxation is close to exponential. This is consistent with the so-called "isotropic" model for librational dynamics, in which uncorrelated librational motions take place simultaneously about the nitroxide *x*-, *y*-, and *z*-axes, but not with those for uniaxial libration [27].

Fig. 10A shows the temperature dependence of the *W*-relaxation parameter for spin-labelled Class I groups, in the presence of 5 M urea; corresponding data for Class II groups are given in Fig. 10C. The *W*-relaxation parameter is calculated from intensity ratios in the low- and high-field intermediate regions (W_L and W_H, respectively), for two fixed delay times $\tau_1 = 168$ ns and $\tau_2 = 296$ ns. This parameter is determined by the product of the mean–square torsional amplitude $\langle\alpha^2\rangle$, and the librational correlation time, τ_C [27]. The temperature profiles of W_L (solid symbols) and W_H (open symbols) are very similar, in each case, showing consistency between the low- and high-field regions of the ED spectra. The two profiles are related by a numerical factor that reflects the different intrinsic sensitivities to angular motion of the high-field and low-field spectral regions. In each case, the librational intensity remains very low up to ca. 180—200 K and increases with increasing temperature beyond this.

3.6. Characterization of librational motion

Fig. 11A shows the temperature dependence of the librational amplitude-correlation time product, $\langle\alpha^2\rangle\tau_c$, for shark and pig kidney Na,K-ATPase labelled on Class I or Class II –SH groups and suspended in 5 M urea. These values are obtained from the measurements of W_L that are given in Fig. 10A and C, by using a conversion factor relating $\langle\alpha^2\rangle\tau_c$ to W_L of 1.0×10^{17} rad^{-2} s^{-2}. A calibration factor with this value was established previously, both for alamethicin spin labelled with TOAC and a phospholipid spin labelled in the lipid chain, by using spectral simulations with the "isotropic" librational model [27,38].

Fig. 11B shows the temperature dependence of the mean–square amplitude, $\langle\alpha^2\rangle$, of the librational motion for the two Na,K-ATPases labelled on Class I or Class II –SH groups. These values are derived from the motionally averaged hyperfine splittings in Fig. 10B and D, according to Ref. [35]:

$$\langle A_{zz}\rangle = A_{zz} - (A_{zz} - A_{xx})\langle\alpha^2\rangle \tag{11}$$

where the angular brackets indicate a motionally averaged hyperfine tensor (of principal elements A_{xx}, A_{yy}, and A_{zz}). From 200 K upwards, the temperature dependence of the librational amplitude is very similar for shark and kidney Class I and Class II groups, in 5 M urea.

Fig. 11C shows the temperature dependence of the rotational correlation time, τ_c, for the librational motion of shark and kidney Na, K-ATPase labelled on Class I or Class II –SH groups and dispersed in 5 M urea. Determinations of the amplitude-correlation time product, $\langle\alpha^2\rangle\tau_c$, from Fig. 11A are combined with the amplitude (i.e., $\langle\alpha^2\rangle$) measurements that are given in Fig. 11B to obtain these values for τ_c. Evaluations are possible only at temperatures above 200 K, for which $\langle\alpha^2\rangle$ is non-zero.

3.7. Three-pulse, stimulated echo-detected EPR spectra

Three-pulse, stimulated-echo ED-EPR spectra are sensitive to motions on the timescale of spin-lattice relaxation (T_1), which is much longer than the phase-memory time (T_{2M}) that determines the timescale for two-pulse, primary echo ED-EPR [26,39]. Fig. 12 shows the three-pulse ED-EPR spectra of shark Na,K-ATPase preparations spin labelled on Class I (left) or Class II (right) –SH groups with 5-MSL, in the presence of 5 M urea. The spectra are recorded at 150 K, 200 K, or 230 K and are given for various values of the second delay time, *T*. They have been corrected for spin-lattice relaxation during the *T*-delay by using inversion recovery measurements, according to Eq. (8). The dependence of the stimulated ED lineshapes on the *T*-delay reveals preferential relaxation in the intermediate spectral regions at low and high field, as for the two-pulse ED spectra, but on the microsecond timescale instead of the nanosecond timescale (see Ref. [26]).

Fig. 13 shows the dependence on *T*-delay of the ED_{SE}^{norm} spectral amplitude at the center of the high-field manifold ($H = 3470$ G). This corresponds to the spectral position that is most sensitive to the angular dynamics. In each case, the high-field amplitude is normalized to the central line height, which is largely insensitive to angular-dependent changes. Least-squares fitting, shown in Fig. 13, reveals single-exponential decays characterized by a time constant, τ_c^*. (An asterisk is used to distinguish the correlation times of the slow motions detected in three-pulse ED-EPR from those of the rapid librations in two-pulse ED-EPR.) Single exponential decays are

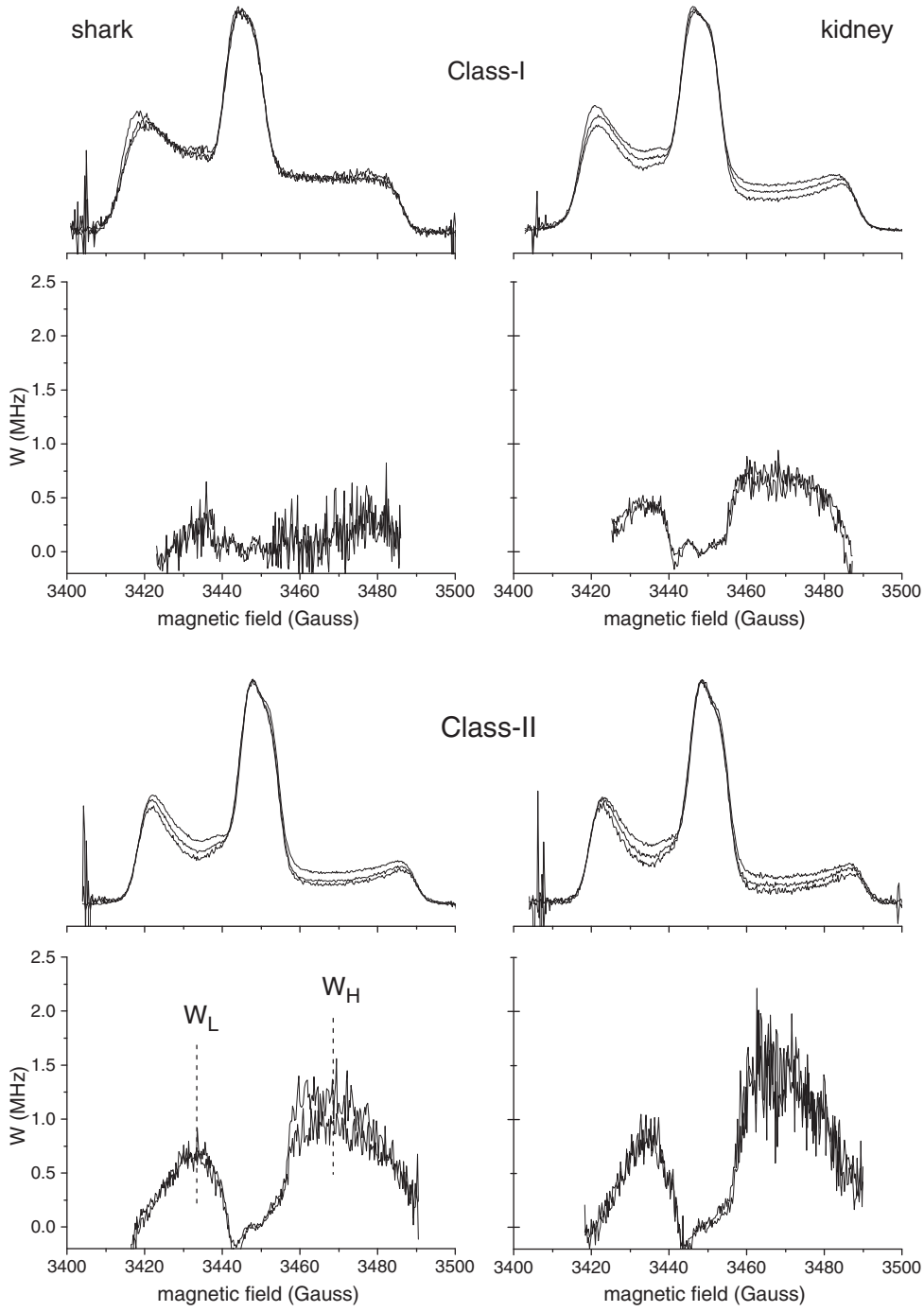

Fig. 9. Two-pulse, echo-detected EPR spectra of Na,K-ATPase membranes from shark salt gland (left-hand side) and pig kidney (right-hand side) labelled on Class I (upper panel) or Class II (lower panel) –SH groups with 5-MSL, in the presence of 5 M urea. $T = 210$ K. ED spectra are recorded for interpulse spacings of (top to bottom) $\tau = 168$, 296, and 424 ns. Spectra are corrected for instantaneous diffusion according to Eq. (6) and are normalized to the central line height. Beneath each spectrum is given the anisotropic part of the relaxation rate, W, obtained according to Eq. (7) from pairs of spectra with interpulse separations of $\tau_1 = 168$ and $\tau_2 = 296$ ns, or $\tau_1 = 168$ and $\tau_2 = 424$ ns.

consistent with a simple two-site model for slow exchange, for which the amplitude of the stimulated echo is given by [26,40]:

$$E(2\tau + T, \Delta\omega) = \frac{1}{2}\, exp\left(-\frac{\tau}{\tau_c^*}\right)\left[(1-\cos\Delta\omega\tau)\, exp\left(-\frac{T}{\tau_c^*}\right) + 1 + \cos\Delta\omega\tau\right] \quad (12)$$

where $\Delta\omega$ is the difference in angular resonance frequency between the two states, and $(2\tau_c{}^*)^{-1}$ is the rate of exchange between states. The values of the single decay times at 150 K, 200 K, and 230 K are given in Table 2. They are all in the microsecond regime and are longer for Class I groups than for Class II groups.

4. Discussion

Conventional CW-EPR shows that, in high concentrations of urea, not all strongly immobilized –SH groups in the Na,K-ATPase are converted to a mobile state that is characteristic of unfolded proteins (Ref. 14, and see Fig. 1). Part of the protein, particularly the transmembrane region, remains folded in the presence of urea. Therefore, the changes that are registered here by ESEEM, ED-EPR, and CW-EPR correspond to only part of the spin-labelled groups. The fractional increase in accessibility to water and reduction in spin–spin interactions, for instance, is therefore considerably larger for the

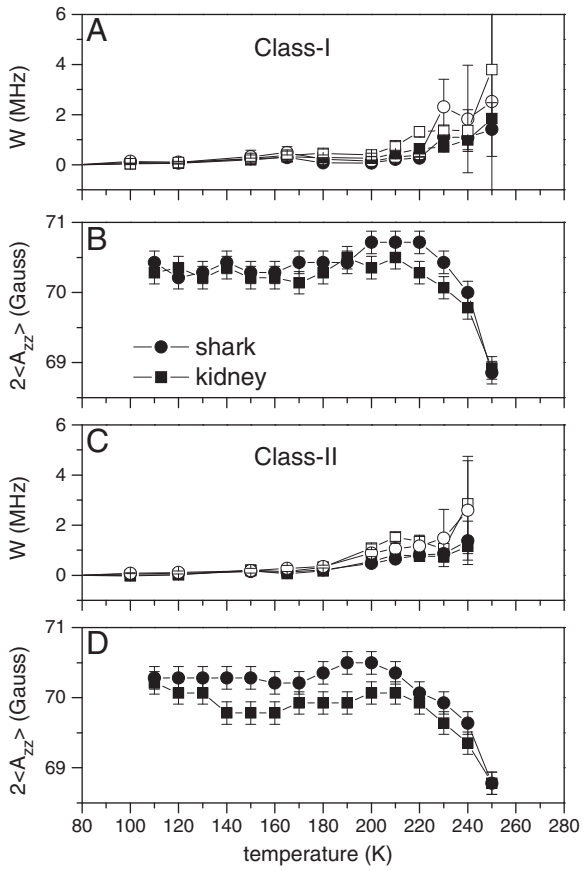

Fig. 10. Temperature dependence of the W_L (solid symbols) and W_H (open symbols) ED-EPR relaxation rate parameters of Class I (A) and Class II (C) groups and of the outer hyperfine splitting, $2\langle A_{zz}\rangle$, in the CW-EPR spectra of Class I (B) and Class II (D) groups, for 5-MSL-labelled shark salt gland (circles) and pig kidney (squares) Na,K-ATPase, in the presence of 5 M urea.

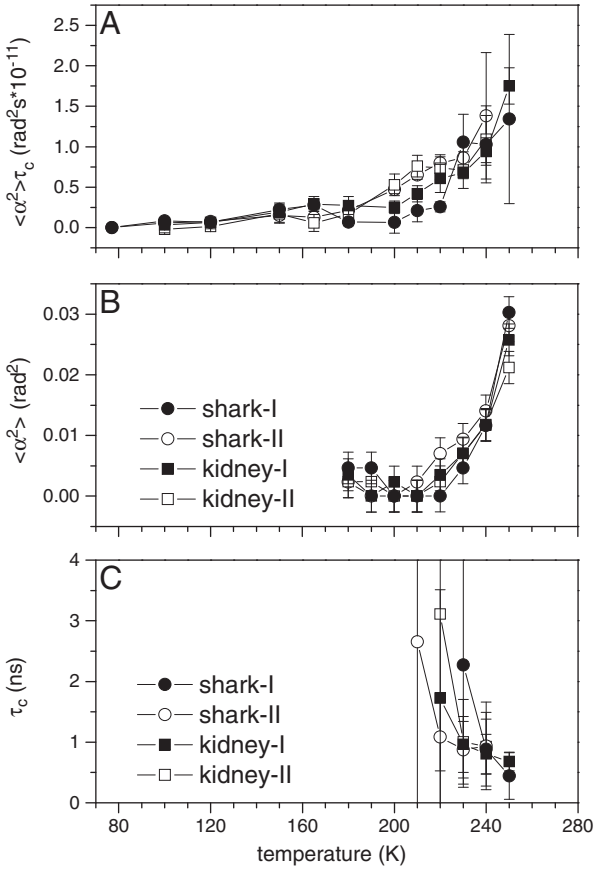

Fig. 11. Temperature dependence of (A) the amplitude-correlation time product, $\langle\alpha^2\rangle\tau_c$ (values are obtained from measurements of the W_L relaxation rate parameter—see Fig. 10); (B) the librational amplitude, $\langle\alpha^2\rangle$ (values are obtained from the motionally averaged hyperfine splitting, $2\langle A_{zz}\rangle$, together with Eq. (11)); and (C) the librational correlation time, τ_c (values are obtained from the amplitude-correlation time product in part A and the librational amplitude in part B). Shark salt gland (circles) or pig kidney (squares) Na,K-ATPase membranes are spin labelled with 5-MSL on Class I (solid symbols) or Class II (open symbols) –SH groups and are suspended in 5 M urea.

unfolded regions of the protein than is indicated by the data for the entire protein in Figs. 2–5. The percentage change in the unfolded regions is more than twice that in these figures.

4.1. Water accessibility

Incubation with urea increases the accessibility of spin-labelled Class I and Class II –SH groups to water for membranous preparations of both shark and kidney Na,K-ATPase (Fig. 3). In the presence of urea, the water accessibility of Class I groups is greater than that of Class II groups, although this is not the case for the enzyme from kidney in the absence of urea. This indicates that enzyme sectors bearing Class I groups are preferentially unfolded by urea, at least in kidney Na,K-ATPase. With 5 M urea, the fractional increase in the narrow D_2O-ESEEM component is much larger than that in the broad component, being 21% and 59% for shark Class I and Class II groups, and 43% and 32% for kidney Class I and Class II groups, respectively. This is because H-bonding to the spin label is disrupted in the presence of urea (cf. Table 1) and, therefore, the narrow D_2O-ESEEM component is a better indicator of the increased exposure to water on protein unfolding than is the broad component.

4.2. Spin–spin interactions

Urea has a greater effect in reducing internal spin diffusion of Class I spin-labelled groups than of Class II groups (Fig. 5). From their rapid kinetics of labelling and intrinsically higher D_2O-ESEEM intensities, the Class I groups are likely to be in the cytoplasmic domain of the protein, rather than embedded in the transmembrane region. Unfolding by urea therefore takes place preferentially in the globular cytoplasmic sector, with concomitant loss in ATPase activity [14] and nucleotide binding capacity (Babavali et al., unpublished). A similar preferential unfolding of the globular domain of the SERCA Ca-ATPase by urea has been found by infrared spectroscopy [11]. Also, calorimetric measurements show that thermal unfolding of the Na, K-ATPase occurs primarily in the cytoplasmic domain, leaving the transmembrane sector relatively intact [41].

4.3. Conformational substates

The heterogeneity in phase-memory times persists to considerably higher temperatures in the presence of urea than in its absence. Single exponential decays are observed at temperatures above 150 K for samples without urea, but not until 210—240 K for samples in 5 M urea (see Fig. 6). A reason for this is that unfolding of the enzyme creates a greater conformational heterogeneity, which is then frozen in at low temperatures. The substates that contribute to this wider conformational spread are not on-pathway and are therefore non-productive. Accordingly, they contribute to the overall loss in enzyme activity that accompanies urea-induced unfolding [14].

On the other hand, the Gaussian distribution widths that are deduced from deconvolution of the low-temperature CW-EPR spectra are only slightly larger in the presence of urea than in its absence (see Fig. 8). Possibly the pronounced Lorentzian narrowing that is induced by urea impacts unfavorably on the sensitivity with which the

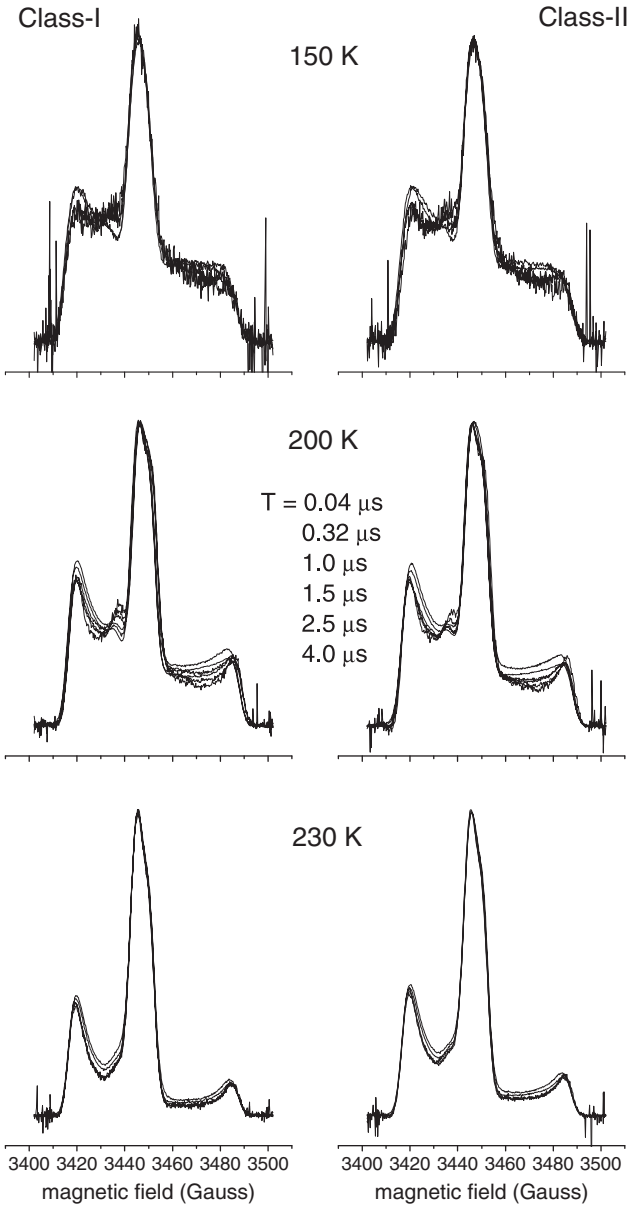

Fig. 12. Three-pulse, stimulated echo ED-EPR spectra of shark rectal gland Na,K-ATPase membranes that are labelled on Class I (left-hand side) or Class II (right-hand side)−SH groups with 5-MSL, in 5 M urea. Temperature: 150 K (top row), 200 K (middle row), and 230 K (bottom row). ED spectra are recorded for fixed τ-delay (216 ns) and increasing (top to bottom) T-delays of 0.04, 0.32, 1.0, 1.5, 2.0, 2.5, and 4.0 μs. Spectra are corrected for spin-lattice relaxation according to Eq. (8) by using inversion recovery ED-EPR spectra recorded at the same temperature and are normalized to the central line height.

deconvolution procedure can determine differences in Gaussian width. Nevertheless, the temperatures at which the Gaussian widths level off to a constant low value in urea are in a range similar to that in which the echo decays first become characterized by a single phase-memory time. This aspect is consistent with the increased conformational heterogeneity in the presence of urea that is deduced from the echo decay curves.

4.4. Rapid librational motion

Comparing with previous measurements on native Na,K-ATPase [16], the extent of torsional libration is increased in the presence of urea (see Fig. 11). At 250 K, the root–mean–square amplitude of librations in 5 M urea increases by ~2° for the shark enzyme labelled

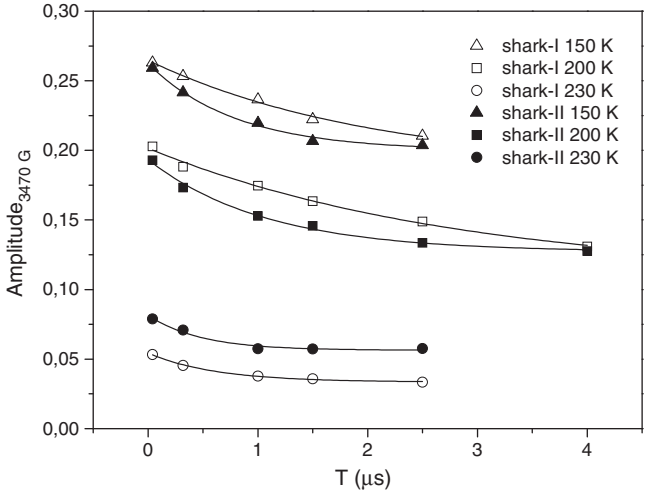

Fig. 13. Dependence on T-delay of the amplitude at 3470-G magnetic field position ($m_I = -1$ manifold) from three-pulse ED-EPR spectra of shark salt gland Na,K-ATPase membranes that are labelled on Class I (open symbols) or Class II (solid symbols) –SH groups with 5-MSL, in 5 M urea. The first interpulse delay is maintained fixed at $\tau = 168$ ns. $T = 150$ K (triangles), $T = 200$ K (squares), and $T = 230$ K (circles). Solid lines are single exponential fits according to Eq. (12).

on Class I or Class II groups and by a comparable amount for the kidney enzyme. Correspondingly, the rate of librational motions, τ_c^{-1}, increases by 40−90%, depending on the temperature. The onset of detectable librational motion also occurs at temperatures that are 10−20 K lower in the presence of urea than in its absence. These are perhaps not massive effects, but they do indicate the tendency of urea to increase the amplitude of fluctuations within conformational substates and to enhance the rate of transitions between them.

4.5. Conformational exchange

In the absence of urea, the larger scale cooperative motions that are detected by three-pulse ED-EPR spectra become greatly retarded at temperatures below the glasslike transition in the Na,K-ATPase, which occurs at just below 200 K [16]. This is seen from the much reduced rates of conformational exchange $(2\tau_c^*)^{-1}$ at 150 K, relative to 200 K, which is evident from the data for 0 M urea that are reproduced in Table 2. In the presence of 5 M urea, however, the rates of conformational exchange at 150 K are not reduced relative to those at higher temperatures (see Table 2). This indicates that the glasslike transition in the protein (if still occurring) is shifted to considerably lower temperature by the action of urea. It is relevant to note here that the "dynamic transition", which occurs in soluble proteins at temperatures around 200 K, is suggested to be coupled to a glass transition in the hydration shell [42], whereas slow "α-fluctuations," which appear in a similar temperature range, are thought to be solvent-slaved motions [43]. Both of these are therefore expected to be affected markedly by the presence of urea.

Table 2
Correlation times, τ_c^*, for slow motion obtained from exponential dependences on T-delay of three-pulse ED_{SE} spectra from shark Na,K-ATPase spin labelled with 5-MSL on Class I or Class II −SH groups, in the presence and absence of 5 M urea.[a]

−SH groups	[Urea] (M)	τ_c^* (μs)		
		150 K	200 K	230 K
Class I	0[b]	9 ± 2	1.26 ± 0.12	–
	5	2.06 ± 0.14	2.85 ± 0.54	0.61 ± 0.27
Class II	0[b]	20 ± 2	0.62 ± 0.01	–
	5	0.80 ± 0.14	1.07 ± 0.15	0.48 ± 0.15

[a] Single-exponential fitting according to Eq. (12).
[b] Data are from Ref. [16].

One of the effects of urea on the CW-EPR spectra is to induce narrowing of the component Lorentzian lines (Fig. 8). This line narrowing can arise partly from reduced spin exchange interactions, as evidenced by the decreased spin diffusion rates (Fig. 5), and also partly from enhanced segmental dynamics in the partially unfolded state. The decrease in Lorentzian half-width is in the range 1−3 G, which would correspond to rates in the 20−55 MHz range if attributed solely to conformational dynamics (cf. 44,45). These upper limits lie between the rates of libration and of conformational exchange that are determined from the two- and three-pulse ED-EPR spectra, respectively. Allowance for the contribution from spin–spin interactions therefore suggests that the dynamic contribution corresponds to intermediate rates of conformational exchange, rather than to fast libration.

5. Conclusion

Both the water accessibility and spin–spin interactions indicate that urea-induced unfolding of Na,K-ATPase takes place principally in the globular extramembranous parts of the protein, as was hypothesized previously [14]. The biochemical significance of conformational substates in soluble proteins is well recognized [17,18] and is found here to apply also to a membrane transport enzyme. Urea has distinct effects on the distribution of conformational substates in the Na,K-ATPase. Conformational heterogeneity is increased, and the glasslike transition in the protein is shifted to lower temperatures. Both are associated with non-productive states that characterize the inactivation of enzyme function by unfolding in urea.

Acknowledgments

We thank Ms. Angelina Damgaard for excellent technical assistance and the Aarhus University Research Foundation for financial support. B.M. gratefully acknowledges support from the Marie Curie Early Stage Training in BIOMEM, grant no. MEST-CT-2004-007931. R.G., R.B., L.S., and D.M. are members of the COST P15 Action of the European Union.

References

[1] J.P. Morth, B.P. Pedersen, M.S. Toustrup-Jensen, T.L.-M. Sørensen, J. Petersen, J.P. Andersen, B. Vilsen, P. Nissen, Crystal structure of the sodium–potassium pump, Nature 450 (2007) 1043–1050.
[2] T. Shinoda, H. Ogawa, F. Cornelius, C. Toyoshima, Crystal structure of the sodium–potassium pump at 2.4 Å resolution, Nature 459 (2009) 446–450.
[3] H. Ogawa, T. Shinoda, F. Cornelius, C. Toyoshima, Crystal structure of the sodium–potassium pump (Na^+, K^+-ATPase) with bound potassium and ouabain, Proc. Natl Acad. Sci. USA 106 (2009) 13742–13747.
[4] J.A. Schellmann, Solvent denaturation, Biopolymers 17 (1978) 1305–1322.
[5] G.I. Makhatadze, Thermodynamics of protein interactions with urea and guanidinium hydrochloride, J. Phys. Chem. B 103 (1999) 4781–4785.
[6] S. Patel, A.F. Chaffotte, F. Goubard, E. Pauthe, Urea-induced sequential unfolding of fibronectin: a fluorescence spectroscopy and circular dichroism study, Biochemistry 43 (2004) 1724–1735.
[7] H. Hong, L.K. Tamm, Elastic coupling of integral membrane protein stability to lipid bilayer forces, Proc. Natl Acad. Sci. USA 101 (2004) 4065–4070.
[8] C.S. Klug, W. Su, J. Liu, P.E. Klebba, J.B. Feix, Denaturant unfolding of the ferric enterobactin receptor and ligand-induced stabilization studied by site-directed spin labelling, Biochemistry 34 (1995) 14230–14236.
[9] C.S. Klug, J.B. Feix, Guanidine hydrochloride unfolding of a transmembrane β-strand in FepA using site-directed spin labeling, Prot. Sci. 7 (1998) 1469–1476.
[10] C.L. Pocanschi, G.J. Patel, D. Marsh, J.H. Kleinschmidt, Curvature elasticity and refolding of OmpA in large unilamellar vesicles, Biophys. J. 91 (2006) L75–L77.
[11] I. Iloro, F.M. Goni, J.L.R. Arrondo, A 2D-IR study of heat- and [C-13]urea-induced denaturation of sarcoplasmic reticulum Ca^{2+}-ATPase, Acta Biochim. Polonica 52 (2005) 477–483.
[12] I. Jorge-García, D.J. Bigelow, G. Inesi, J.B. Wade, Effect of urea on the partial reactions and crystallization pattern of sarcoplasmic reticulum adenosine triphosphatase, Arch. Biochem. Biophys. 265 (1988) 82–90.
[13] M. Esmann, Sulfhydryl groups of $(Na^+ + K^+)$-ATPase from rectal glands of *Squalus acanthias*—titration and classification, Biochim. Biophys. Acta 688 (1982) 251–259.
[14] M. Babavali, M. Esmann, N.U. Fedosova, D. Marsh, Urea-induced unfolding of Na,K-ATPase as evaluated by electron paramagnetic resonance spectroscopy, Biochemistry 48 (2009) 9022–9030.
[15] R. Bartucci, D.A. Erilov, R. Guzzi, L. Sportelli, S.A. Dzuba, D. Marsh, Time-resolved electron spin resonance studies of spin-labelled lipids in membranes, Chem. Phys. Lipids 141 (2006) 142–157.
[16] R. Guzzi, R. Bartucci, L. Sportelli, M. Esmann, D. Marsh, Conformational heterogeneity and spin-labelled-SH groups: pulsed EPR of Na, K-ATPase, Biochemistry 48 (2009) 8343–8354.
[17] H. Frauenfelder, F. Parak, R.D. Young, Conformational substates in proteins, Ann. Rev. Biophys. Biophys. Chem. 17 (1988) 451–479.
[18] H. Frauenfelder, G. Chen, J. Berendzen, P.W. Fenimore, H. Jansson, B.H. McMahon, I.R. Stroe, J. Swenson, R.D. Young, A unified model of protein dynamics, Proc. Natl Acad. Sci. USA 106 (2009) 5129–5134.
[19] I. Klodos, M. Esmann, R.L. Post, Large-scale preparation of sodium–potassium ATPase from kidney outer medulla, Kidney Int. 62 (2002) 2097–2100.
[20] J.C. Skou, M. Esmann, Preparation of membrane-bound and of solubilized $(Na^+ + K^+)$-ATPase from rectal glands of *Squalus acanthias*. The effect of preparative procedures on purity, specific and molar activity, Biochim. Biophys. Acta 567 (1979) 436–444.
[21] O.H. Lowry, N.J. Rosebrough, L. Farr, R.J. Randall, Protein measurement with the Folin phenol reagent, J. Biol. Chem. 193 (1951) 265–275.
[22] M. Esmann, ATPase and phosphatase activity of the Na^+, K^+-ATPase; molar and specific activity, protein determinations, Methods Enzymol. 156 (1988) 105–115.
[23] M. Esmann, Sulfhydryl groups of $(Na^+ + K^+)$-ATPase from rectal glands of *Squalus acanthias*: detection of ligand induced conformational changes, Biochim. Biophys. Acta 688 (1982) 260–270.
[24] D.A. Erilov, R. Bartucci, R. Guzzi, A.A. Shubin, A.G. Maryasov, D. Marsh, S.A. Dzuba, L. Sportelli, Water concentration profiles in membranes measured by ESEEM of spin-labeled lipids, J. Phys. Chem. B 109 (2005) 12003–12013.
[25] R. Bartucci, R. Guzzi, L. Sportelli, D. Marsh, Intramembrane water associated with TOAC spin-labelled alamethicin: electron spin-echo envelope modulation by D_2O, Biophys. J. 96 (2009) 997–1007.
[26] D.A. Erilov, R. Bartucci, R. Guzzi, D. Marsh, S.A. Dzuba, L. Sportelli, Echo-detected electron paramagnetic resonance spectra of spin-labeled lipids in membrane model systems, J. Phys. Chem. B 108 (2004) 4501–4507.
[27] D.A. Erilov, R. Bartucci, R. Guzzi, D. Marsh, S.A. Dzuba, L. Sportelli, Librational motion of spin-labeled lipids in high-cholesterol containing membranes from echo-detected EPR spectra, Biophys. J. 87 (2004) 3873–3881.
[28] F. De Simone, R. Guzzi, L. Sportelli, D. Marsh, R. Bartucci, Electron spin-echo studies of spin-labelled lipid membranes and free fatty acids interacting with human serum albumin, Biochim. Biophys. Acta 1768 (2007) 1541–1549.
[29] Yu.V. Toropov, S.A. Dzuba, Yu.D. Tsvetkov, V. Monaco, F. Formaggio, M. Crisma, C. Toniolo, J. Raap, Molecular dynamics and spatial distribution of TOAC spin-labeled peptaibols studied in glassy liquid by echo-detected EPR spectroscopy, Appl. Magn. Reson. 15 (1998) 237–246.
[30] K.M. Salikov, Y.D. Tsvetkov, Electron spin–echo studies of spin–spin interactions in solids, in: L. Kevan, R.N. Schwartz (Eds.), Time Domain Electron Spin Resonance, Wiley-Interscience, New York, 1979, pp. 231–278.
[31] R. Bartucci, R. Guzzi, D. Marsh, L. Sportelli, Chain dynamics in the low-temperature phases of lipid membranes by electron spin-echo spectroscopy, J. Magn. Reson. 162 (2003) 371–379.
[32] J.R. Klauder, P.W. Anderson, Spectral diffusion decay in spin resonance experiments, Phys. Rev. 125 (1962) 912–932.
[33] D. Marsh, Polarity contributions to hyperfine splittings of hydrogen-bonded nitroxides—the microenvironment of spin labels, J. Magn. Reson. 157 (2002) 114–118.
[34] D. Kurad, G. Jeschke, D. Marsh, Lipid membrane polarity profiles by high-field EPR, Biophys. J. 85 (2003) 1025–1033.
[35] S.P. Van, G.B. Birrell, O.H. Griffith, Rapid anisotropic motion of spin labels. Models for motion averaging of the ESR parameters, J. Magn. Reson. 15 (1974) 444–459.
[36] S.A. Dzuba, Yu.D. Tsvetkov, A.G. Maryasov, Echo-detected EPR spectra of nitroxides in organic glasses: model of orientational molecular motions near equilibrium position, Chem. Phys. Lett. 188 (1992) 217–222.
[37] S.A. Dzuba, Librational motion of guest spin probe molecules in glassy media, Phys. Lett. A 213 (1996) 77–84.
[38] R. Bartucci, R. Guzzi, M. De Zotti, C. Toniolo, L. Sportelli, D. Marsh, Backbone dynamics of alamethicin bound to lipid membranes: spin-echo EPR of TOAC spin labels, Biophys. J. 94 (2008) 2698–2705.
[39] S.A. Dzuba, E.P. Kirilina, E.S. Salnikov, L.V. Kulik, Restricted orientational motion of nitroxides in molecular glasses: direct estimation of the motional time scale basing on the comparative study of primary and stimulated electron spin echo decays, J. Chem. Phys. 122 (2005) 094702-1–094702-7.
[40] G.M. Zhidomirov, K.M. Salikov, Contribution to theory of spectral diffusion in magnetically diluted solids, Sov. Phys. JETP 29 (1969) 1037.
[41] E. Fodor, N.U. Fedosova, C. Ferencz, D. Marsh, T. Páli, M. Esmann, Stabilization of Na, K-ATPase by ionic interactions, Biochim. Biophys. Acta 1778 (2008) 835–843.
[42] W. Doster, The dynamical transition of proteins, concepts and misconceptions, Eur. Biophys. J. 37 (2008) 591–602.
[43] P.W. Fenimore, H. Frauenfelder, B.H. McMahon, R.D. Young, Bulk-solvent and hydration-shell fluctuations, similar to α- and β-fluctuations in glasses, control protein motions and functions, Proc. Natl Acad. Sci. USA 101 (2004) 14408–14413.
[44] L.I. Horváth, P.J. Brophy, D. Marsh, Exchange rates at the lipid–protein interface of myelin proteolipid protein studied by spin-label electron spin resonance, Biochemistry 27 (1988) 46–52.
[45] L.I. Horváth, P.J. Brophy, D. Marsh, Microwave frequency dependence of ESR spectra from spin labels undergoing two-site exchange in myelin proteolipid membranes, J. Magn. Reson. B 105 (1994) 120–128.